# Frontal and temporal lobe sources for a marker of controlled auditory attention:
# the negative difference (Nd) event-related potential.

Boutheina Jemel[1] (PhD), Robert D. Oades (PD), Ljubov Oknina (PhD), Christiane Achenbach (MB),
Bernd Röpcke (Dr rer medic),

University Clinic for Child and Adolescent Psychiatry and Psychotherapy, Virchowstr. 174, 45147
Essen, Germany

**Abstract:**

Frontal and temporal lobe sources for electrical activity associated with auditory controlled attention (negative difference, Nd) were sought for comparison with those reported to arise from the earlier detection of stimulus-change (mismatch negativity, MMN: Jemel et al. 2002). In two sessions a month apart (T1 and T2), 14 subjects were presented with a 3-tone oddball passively, then as a discrimination. In EEG recordings (32 sites), Nd was calculated by subtraction of the event-related potential elicited by a non-attended stimulus from that after the same frequency-deviant as target. Putative generators in the 180-228 ms latency-range were modelled with brain electrical source analysis and mapped to the modified Montreal brain-atlas. Initial T1-analyses located bilateral Nd dipoles in the superior temporal gyrus (BA22) and the dorsolateral prefrontal cortex (BA8). Re-test allowed estimates of the temporal and spatial extension of activity. Peak activity occurred 14 ms later. Step-by-step analysis showed that the best spatial fit for the inverse-solutions extended 3-6 mm from the point sources, but for temporal lobe sources this increased 15 mm caudally. The right mid-frontal source (BA10) was rostral and ventral from that in the left superior frontal gyrus (BA8). T1 and T2 dipole strengths were well correlated. Nd measures of controlled attention localised to areas associated with sustained attention, problem-solving and working-memory. Temporal lobe sources were later and more posterior and medial than for automatic change-detection. Frontal Nd sources were more dorsal on the right and more rostral on the left than MMN dipoles reported for the right inferior frontal and left anterior cingulate. The sequence of information processing is reviewed.

**Key words:**

| | | | |
|---|---|---|---|
| Auditory event-related potential | Attention | Dipoles | Frontal lobe |
| MMN    Negative difference | Temporal lobe | | |

**INTRODUCTION**

Event-related potential measures (ERPs) of auditory changes based on sensory memory (mismatch negativity, MMN) and of voluntary selective attention (negative difference, Nd) rep-resent pre- and post-conscious processes and are well-suited as measures of automatic and controlled processing, respectively (Giard et al. 2000; Woods et al. 1993).

Nd is a form of processing negativity revealed by the subtraction of an ERP elicited by an unattended tone from that recorded when the same tone is attended (e.g. a discrimination target). Processing negativity is a generic term for subtraction waveforms that reveal target-related processing. Nd is the

more precise measure making use of the same physical stimulus with and without attention directed to it. N2b is another example based on the subtraction of waveforms elicited by the target minus the standard. N2b typically peaks later than the Nd component described here and has been studied in a time window that starts where the Nd under study here stops (Kasai et al. 2002; Sussman et al. 2002).

The earlier of two main Nd components peaks about 200 ms post-stimulus, predominantly at fronto-central electrodes (Hansen and Hillyard, 1980). This subtraction procedure controls for all stimulus features except "target-ness" (the differential processing of attended and unattended channels) and possible momentary changes in the state or direction of attention. Nd is thus a specific marker for a to-be-attended class of stimulus, the so-called attentional trace (Hansen and Hillyard, 1983; Näätänen, 1988; Oades et al. 1997). Functionally, it seems to reflect either a *match* with the template for what the target is or a *mismatch* with other stimuli perceived to be non-meaningful. (More recently the earlier and later components have been related respectively to functions of stimulus set [Hillyard and Picton, 1988] and to rehearsal of the attentional trace or set [Kasai et al. 2001]).

These features of the Nd contrast with those for the MMN that peaks earlier (100 to 200 ms post-stimulus) and likely reflects the *mismatch* with a template for the perceptual features of repeated standard tones elicited by a non-target deviant (Cowan et al.1993). The function of MMN (change detection) may be said to reflect the process necessary to effect a switch of attention (Escera et al. 2000a,b) to allow adaptive response to a potentially significant event. The function of Nd (relevance detection) reflects the need to switch attention to a stimulus that is in some sense rewarding, relevant and in need of further processing (Näätänen, 1988).

Both ERP components reflect successive enhancement mechanisms along the processing path. These may be conceptualised as volume-control or sensory-gain for stimuli in terms of salience (for MMN) or reinforcement parameters (for Nd). Both

mechanisms, automatic and controlled, reflect the selection of information for further processing. Thus both are attentional in the sense that they represent the 'selective aspect of perception' (Treisman, 1969). Further, both indicate attentional effects in sensory areas that reflect re-activation or enhancement from higher order brain regions, as in other sensory modalities (Kastner and Ungerleider, 2000)

Few have investigated the potential frontal and temporal lobe generators for these pre- and post-conscious processes and none have differentiated sources for sequential automatic and controlled processing using brain atlas coordinates. Our aim is to compare the locus and activation sequence of MMN generators (Deouell et al.1998; Waberski et al. 2001; Jemel et al. 2002) with those reported here for Nd. Studies with brain-damaged patients and source-modelling proposed sources (without coordinates) for early Nd components in the temporal lobe and later ones in the frontal cortex (Giard et al. 2000; Kasai et al. 1999; Woods et al. 1993). Neuroimaging studies have implicated several frontal loci (including inferior frontal gyrus and cingulate cortex [Kounios et al. 2001]) where MMN sources are reported (Jemel et al. 2002; Waberski et al. 2001). But they necessarily use different conditions and lack the temporal resolution of ERP studies. Indeed, these presentations confuse the areas mediating sound discrimination with those involved in change-detection.

This investigation concentrates on an active auditory discrimination and Nd, for which central coordinates have not been reported. We hypothesize that one of the frontal Nd generators would occur not far in time and space from the late frontal MMN dipole (Jemel et al. 2002) that is presumably involved in an executive or switching role in the flow of information processing (Escera et al. 2000a,b). But, we have no a priori reason for predicting the temporal order of activation of the later dipoles (successive or simultaneous). The flow of top-down in put to the temporal regions is predicted to involve areas posterior to those initially involved in MMN registration reflecting the involvement of "higher" associative functions. We shall

discuss a proposal to relate the temporal sequence of processing functions represented by MMN and Nd dipole activity.

## MATERIALS AND METHODS

### Subjects and Stimuli

Data were analysed from 9 male and 5 female healthy right-handed volunteers (aged 21-36 years). They attended two recording sessions about one month apart. None had a history of neurological or psychiatric illness or used drugs affecting the central nervous system. They were tested for normal hearing (BCA audiometer) and had normal or corrected-to-normal vision. Following agreement of the clinic ethics committee to the protocol subjects provided written consent to participate.

All stimuli were generated with Neuro-Stim software. A binaural 3-tone oddball presentation consisted of sinusoidal tones (76 dBspl: Dippacher TDH 39 earphones) where standards had a frequency of 1 kHz (Std.: p = 82%, duration 80 ms including 10 ms rise and fall times), frequency-deviants (targets) had the same duration but a frequency of 1.5 kHz (Fd: p = 6%) and duration deviants (non-targets) had the frequency of the Std but lasted only 40 ms (Dd: p = 6%). Thus the stimulus onset asynchrony (SOA) varied from 1040 to 1080 ms. Complex novel sounds (p = 6%) were also presented but are not considered in the present analysis. There were 400 tones in each of the 4 blocks of trials presented in the auditory passive and the following auditory discrimination. Subjects were asked in the second condition to respond to the Fd with a button press alternately between blocks with the right and left hand, to watch the screen but to ignore all other visual and auditory stimuli.

Salient deviants were chosen to produce large amplitudes with more reliable test-retest sensitivity and signal-to-noise ratios for localisation. A binaural rather than dichotic presentation was used to enable the bilateral localization and activation sequence of the dipoles. A relatively long SOA was chosen to satisfy the requirements of making a multi-stimulus discrimination. The stimulus presentation order was pseudo-random with each deviant preceded by at least one Std.

In the first (auditory passive) condition red and green circles were presented (50:50) for discrimination in order to record the non-attended Fd ERP for Nd calculation. Each subtended an angle of 3.8° at 1.5 m and alternated at random every 1100 ms on a PC screen. Subjects responded alternately between blocks with the left and right hand to the green circle. The visual presentation in the second condition (auditory discrimination) provided a perceptual balance for the discrimination in the first condition. The onsets of the visual and auditory stimuli were controlled so that they did not coincide. This procedure was the same in the two sessions conducted one month apart.

### EEG recording

The EEG was recorded from 29 channels placed in an extended 10-20 system. These were the Fz, Cz, Pz, Oz, F7, F3, F4, F8, C3, C4, P3, P4, T3, T4, T5, T6 and the left and right mastoids, along with Fpz, FCz, CPz on the longitudinal axis, FT7-FT8 over the fronto-temporal, FC3-FC4 over the fronto-central, CP3-CP4 over the centro-parietal and TP7-TP8 over the temporo-central regions. A vertical and horizontal EOG was recorded from the supraorbital ridge and the outer canthus of the right eye to monitor blink- and eye-movements for offline rejection of artefacts (>50 μV). Linked ear-lobes were used as a reference. The use of the nose- and the average-reference were recomputed off line. The EEG signal (impedance < 5kOhm) was amplified using a SynAmps amplifier with a bandpass of 0.1–100 Hz, was digitised with 16-bit resolution, sampled at 500 Hz and stored on a hard disk. Records were epoched separately for each tone type (100 ms pre-stimulus period for the baseline adjustment to 800 ms post-stimulus onset), and digitally filtered offline (30 Hz low-pass, 24-dB/octave). Grand means for each deviant (96/block) were based on about 1120 sweeps reflecting rejection rates of 2% for errors and 5-15% for artefacts (see Figure 1).

### Data analysis

Three ERP components were defined by peaks at Fz, FCz and Cz: a) the N1 in the

stimulus-elicited waveform (80-140 ms), b) the MMN (100-200 ms) in the non-target-deviant-minus-standard wave-form, and c) the Nd (150-300 ms) formed by subtraction of the non-target Fd in passive auditory presentations from the target Fd in the active auditory discrimination. Separate statistical analyses were run for each component. Initially, waveforms were compared within subjects using a two-way ANOVA for midline sites for the factors deviant (Fd *vs*. Dd) and electrode (Fz, FCz, Cz), and a 3-way ANOVA with session, deviant (Fd *vs*. Dd), and laterality (F7-F8, FT7-FT8, FC3-FC4, C3-C4) as factors. Greenhouse-Geisser corrected F-values were used and significant inter-actions were clarified with the univariate F contrasts reported. The present analysis concentrates on a comparison of dipole strengths and latencies using paired t-tests. Pearson correlation coefficients were calculated for between-session ERP measures and for within and between session dipole measures.

We compared a brain electrical source analysis (BESA, [Scherg and Berg, 1991]) of dipoles for Nd, from which stereotaxic Talairach coordinates could be calculated with software developed by Garnero et al. (Crottaz-Herbette and Ragot, 2000) and placed on the modified Montreal brain atlas.

Dipole computation was based on a time window (-50 to + 500 ms) and low-pass filtered to avoid aliasing (14 Hz, 24 dB/octave). Dipole calculations based on topographic potentials require an independent reference. For this the average reference was used, that takes in to account the variations of potential at any single recording site (Lehmann and Skrandies, 1984; Nunez, 1981; Nunez et al. 1994; Pasqual-Marqui and Lehmann, 1993). Potential maps were computed with a spline interpolation algorithm, and the data presented as scalp current density maps (SCD: the second spatial derivative of the potential) to enhance the focal sources (Pernier et al. 1988). This technique was used to provide information on the approximate number and position of ERP generators. It emphasizes local contributions to the surface map, providing a better visualization of the approximate locations of intracranial generators, without the influence of the reference electrode (e.g.

figure 2). But it should be borne in mind that it emphasizes superficial sources relative to more distant, subcortical sources (Pernier et al. 1988).

BESA source-modeling allows iterative fitting of the dipole location and orientation in a spherical head-model with an inner radius of 85 mm corrected for brain, skull, and scalp conductivity (Scherg and Picton, 1991), until the difference between the recorded surface data and the calculated surface data of the dipole-model is minimised (least square fit). The principal components analysis showed that 4 dipoles would explain the data recorded in the Nd time window. This matched the requirement that the maximum number of calculable equivalent current dipole sources is obtained by the number of electrodes divided by six. This requirement is based on the consideration that each dipole has 6 parameters (3 for location, 2 for orientation and one for dipole strength). The present analysis thus lies well within these empirical constraints. In addition, we have more degrees of freedom avail-able, for the results showed that the temporal lobe sources were symmetrical. This means that the parameter location was fixed for two dipoles (Kamijo et al. 2002; Picton et al. 1995).

The goodness of fit is expressed by the residual variance (RV) as a percentage of the signal variance. Each model was hypothesis-led (e.g. Jemel et al. 2002) and first fitted to the ERP grand mean (session 1), that describes the most reliable characteristics of the spatio-temporal data matrix, and then applied to the individual subjects' data as a test of the stability of the solution. This model was replicated with the grand mean and the individual ERPs in the second session.

**RESULTS**

*The Nd Waveform*

We restricted the statistical analysis to the major (mid-late) component of the Nd waveform (Nd2 or Ndl) at 8 fronto-central sites shown in fig. 1. The mean maximum negative amplitude was recorded at FCz (-7.1 ± 4.1 µV). There were no significant differences for lateral sites or between

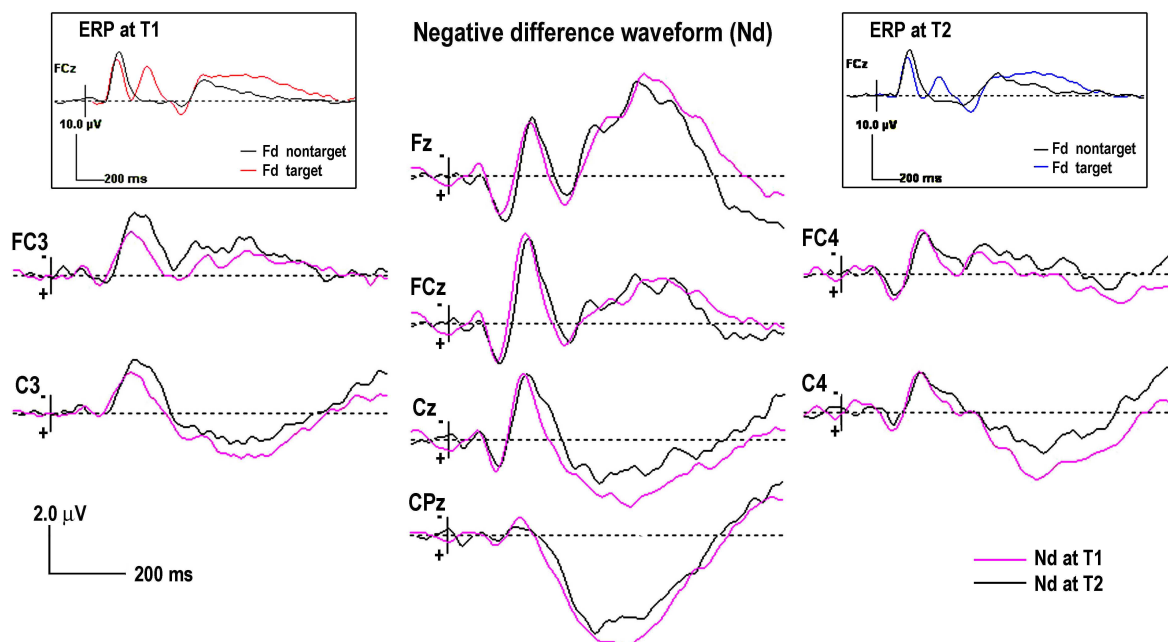## Stimulus-elicited and subtraction waveform



**Figure 1**

Nd waveforms over 8 fronto-central electrode sites with average-reference for sessions T1 and T2, respectively. The inserted frames show the ERP raw waveforms elicited by the attended and non-attended frequency deviant tones for T1 (top left) and T2 (top right). The peak Nd latencies at FCz were 205 (T1) and 219 ms (T2). [The mean target reaction times were 438 / 436 ms; errors of commission 0.5 / 0.07 and errors of omission 4.4 / 1.9 for T1 and T2, respectively.]

sessions. Positive mastoid peaks were larger than at T5/T6 (electrode F (1, 13) = 15.96, p <.002, data not shown). Individual peak latencies ranged from 184 to 228 ms: these did not overlap with N1 nor differ across sites, but the mean peak latency increased on session 2 vs. session 1 (e.g. FCz, 205-219 ms ± 11-17, $F_s$ [1, 13] > 9.88, $p_s$ <.008: fig. 1). Significant correlations between the two sessions for these 8 sites were obtained for amplitude (from r = .56 at Fz to .69 at FC3), but not for latency at 7 of the 8 sites (from r = .19 at Fz to .51 at Cz).

### *Dipole analysis – session 1*

The principal components analysis of BESA showed that 4 components (dipole sources) were necessary to explain all the topographic data. Attempts to fit the N1 and MMN 4-dipole-solutions (Jemel et al. 2002) with adjustments in the time-window covering the Nd (180-228 ms) resulted in very high RV (ca.30 %).

We then examined the SCD time course (Nunez et al. 1994). Figure 2 shows the

development of the SCD for Nd at early-, mid- and late latencies (182, 204 and 220 ms respectively). This illustrates negative current sinks with a positive current source indicative of tangential generators in the general region of the central sulcus, and temporal lobe current sinks with a broad frontal positive current source. This suggested two more radial generators in the posterior superior temporal plane and frontal lobe. These loci recall a report on two Nd components associated with a fronto-supplementary motor and a superior parietal region (Dien et al. 1997). Thus, to model the Nd in session 1 (with similar time-window adjustments), 4 dipoles were iteratively fitted within the temporal and frontal areas in each hemisphere both to reduce the RV, and to obtain a maximum match for the dipoles' activity with the data giving the SCD scalp distribution.
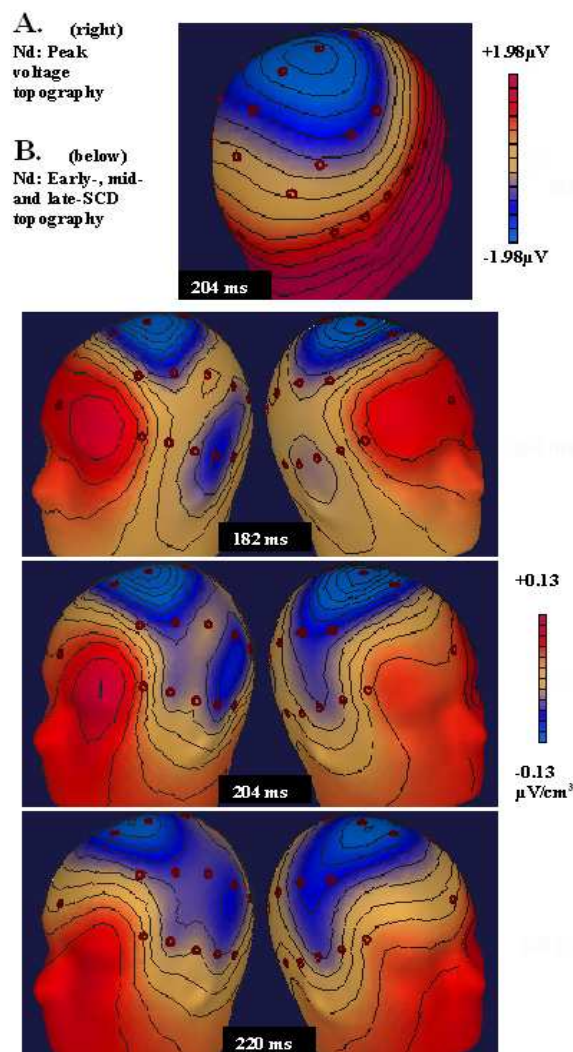
**A.** (right)
Nd: Peak voltage topography

**B.** (below)
Nd: Early-, mid- and late-SCD topography

+1.98 µV

-1.98 µV

204 ms

182 ms

+0.13

-0.13 µV/cm³

204 ms

220 ms

**Figure 2**
A/ A topographic map of the Nd voltage scalp distribution near the peak latency.
B/ Development of source current density (SCD) representations of the Nd over the period that the Nd event-related potential was negative: at the start (182 ms), around the peak (212 ms) and at the end (232 ms).

Starting from different loci identical solutions were obtained for the locations of these 4 dipoles in the time window from the earliest to the latest Nd peak (180-228 ms). The mean RV for the 4-dipole constrained solution was 0.9 % with a best peak value of 0.6% (Fig. 3 on the left). Applying this model to the individual subjects' data resulted in a mean RV of 5.6% (SD 2.78), where 4 values were < 2.9% and the least good fit was 10.3%.

The auditory cortical sources within 3 mm of the calculated point dipole were located in the grey matter of the superior temporal gyrus (Brodmann area [BA] 22, x ±31, y -50, z +19) and the frontal lobe sources were located in the grey matter on the border of the superior and middle frontal gyri (BA 8, x ±26, y +28, z +47, Fig. 3, left and 4 top). The right frontal locus was activated first (186 ms), followed by that on the left (202 ms) with both peaking earlier than the two temporal lobe sources (208-218 ms: t = 3.14 to 3.89, p = .002-.008: fig. 3). Frontal dipoles were stronger than either of the temporal lobe sources (on the right t = -2.31, p = .03, on the left t = -1.9, p = .08: see fig. 3).

***Dipole analysis – replication in session 2: the time-window dimension***

This solution for session 1 was applied to the data from session 2 obtained a month later. For some subjects this gave a similarly good fit (RV of 1.7%; best peak result of 1.1%), but the group RV was 5%. Using this solution for session 1 and 2 resulted in significant differences for the fit (RV: t =-3.91, p = .002). As reported above, the Nd peak latency was a bit longer on session 2. Using a 5 ms later window improved the RV to 3.5%. Thus it was appropriate, as a test of accuracy for the session 1 solution to re-model using the same spatial solution as the *a priori* hypothesis for a later latency window. The solution improved, resulting in a mean RV of 1.8% (best fit 0.9%) for the window of 185-230 ms (table I).

In the frontal lobe (x +3.6, y +3.1, z +2.4 and x −2.2, y +1.6, z +5.1) the loci for the second solution were 4-5 mm more lateral on the right and less lateral on the left. They were marginally more rostral on the right, but about 10 mm more caudal on the left, and some 20 mm less dorsal on the right, but 4 mm more dorsal on the left. Thus both dipoles remained in the mid-frontal gyrus, but sources were closer to BA 9 on the right and BA 6 on the left.

For the temporal lobe, the bilateral solutions were a mere 3 mm more lateral and 6 mm more dorsal; however they were 20 mm more posterior within the mid-temporal gyrus close to the temporo-occipital border (x ±34, y -70, z +25: BA 39).
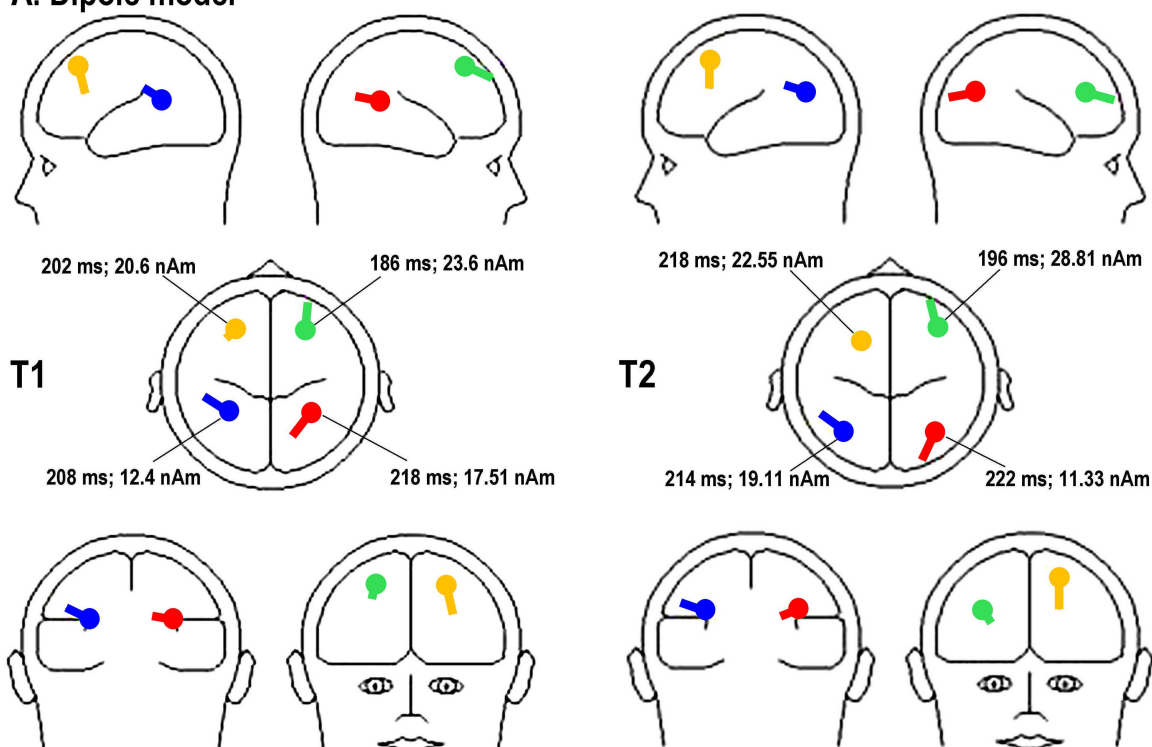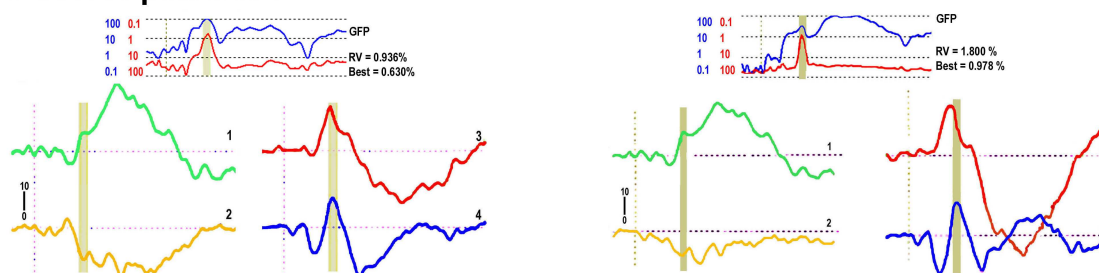
**Figure 3**

A/ Spherical head model (BESA) views of the locations of the 4-dipole solutions for the Nd waveform in the first T1 and the second T2 sessions from the side (top of figure), above (mid-figure) and frontal/rear views (bottom of the figure). The peak latencies and peak strengths of the dipoles are given in the middle of the figure. B/ Waveforms for the 4 dipoles (below) where the shaded bar represents the time window studied. Above, progress over time for the global field power as recorded (blue) and modelled (red), where the difference reflects the residual variance (RV) of the data recorded remaining unexplained by the model. The RV values in the text refer to the mean across the window, with the best fit representing the peak

The differences between the two solutions may have reflected either the accuracy of modelling the inverse solution and/or that there was a spread of activation that was more extensive than the point sources identified by the models. The latter explanation seems plausible considering the slightly later latency window. Further, evidence for the latter explanation may be derived from the highly significant correlations obtained between the two solutions for RV (r =.89, p <.0001), the amplitudes of the 4 dipoles (r = .73-.88, p = .0001-.005) and latency (r = .53-.77, p = .002-.065). We therefore examined the spread of the spatial area that presented a stable solution with a good fit in more detail.
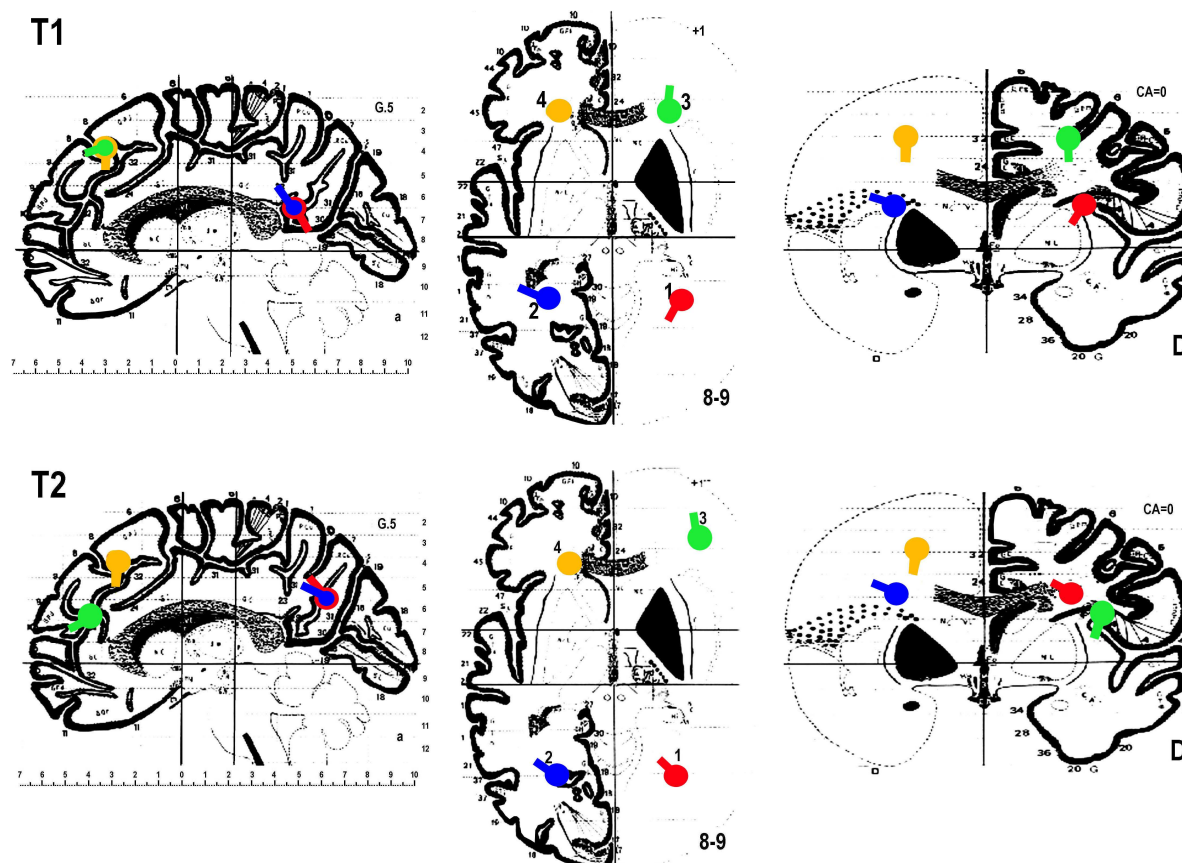
**Figure 4**
The dipole-sources of the Nd waveform in response to target frequency-deviant tones in the first T1 and second T2 recording sessions are shown in sagittal, coronal and axial views of maps from the modified Montreal brain atlas. Superior temporal gyral sources extend posteriorly from the parietal (T1) to the occipital lobe borders (T2). The frontal lobe sources were located on the right in the mid-frontal gyrus and on the left in the superior frontal gyrus (See T2 maps). The T1 locations reflect a forced average under constraints of forced inter-hemispheric symmetry.

### *Dipole analysis – replication in session 2: the volume dimension*

We investigated the possibility that Nd activates an extensive region of the temporal lobe (in the secondary auditory cortex extending to the medial temporal lobe and temporal-occipital junction) and the frontal lobe (across BA 6, 8 and 9 on the borders of the superior and medial frontal gyri).

The extent of the spatial dimensions for a good explanation of frontal activity was explored first. Initially, to explain the data distribution recorded in session 2, we fixed symmetric dipoles according to the session 1 solution, and then moved them in 12-14 steps of one unit on the BESA coordinates. This corresponded to ca. 5% (theta dimension) to 10% (ecc and phi dimensions) of each of the 3 dimensions. This resulted in changes of 1-5 mm (x-axis), 3-8 mm (y-axis) and 0-7 mm (z-axis) before unstable solutions arose (RV range 2.2-2.5%). Minimal RV (2.2%) was obtained at x 24, y 25 and z 43. Setting one dipole free to move, but requiring symmetry contralaterally (including the temporal dipoles) resulted in frontal coordinates of x 23, y 29, z 30 and temporal lobe coordinates of x 29, y 58 and z 29 (table I).

The dipoles were then set free from symmetry constraints to test whether the constrained analysis (above) reflected the likely physiological distribution of activity. For frontal sources this improved the solution further (RV = 1.1%). For this final solution the right frontal sources coordinates were x +36, y +33 and z +20 (BA 10, mid-frontal gyrus), while in the left hemisphere they were x −23, y +24 and z +47 (BA 8, superior frontal gyrus: fig. 4, right).

**Table I:**

**Coordinate variations with successive dipole-solutions (with respect to condition T1, T2 – see text for details): units mm**

| Model | Frontal lobe | | | Temporal lobe | | | Residual variance |
|---|---|---|---|---|---|---|---|
| | x | y | z | x | y | z | RV   % |
| T1 solution | ±26 | +28 | +47 | ±31 | -50 | +19 | 0.9 % |
| T1 to T2 | | | | | | | 5.0 % |
| Modify time window | ±24 | +25 | +43 | ±29 | -58 | +29 | 3.5 % |
| Free frontal dipole | -22/+36 | +16/+31 | +51/+24 | ±34 | -70 | +25 | 1.8 % |
| Solution range step-by-step (mm) | 5 | 8 | 7 | 36 | 40 | 1 | ±1 % |
| Re-model free frontal dipole | -23/+36 | +24/+33 | +47/+20 | ±31 | -50 | +19 | 1.1 % |
| Solution range step-by-step (mm) expressed as coordinates | 5 / 5 | 3 / 4 | 2 / 5 | 23 | 31 | 5 | ±1% |
| | -19 to-24 +34 to +39 | +24 to +27 +33 to +38 | +47 to +49 +16 to +22 | ±21-44 | +40 to +71 | +23 to +28 | |

[The asymmetric frontal sources were also examined by a step-by-step analysis fixing left and right dipoles in turn (as described above). RV remained no more than 1.4-1.5% for variations of 3-5 mm in the three spatial dimensions (The coordinates and RV for the successive dipole solutions are given in table I).]

Temporal lobe source coordinates under the condition of asymmetric frontal sources were x ±31, y −50 and z +19 (BA 39: parietal-occipital border). There was no stable solution for these dipole coordinates when sources were freed from constraints. From this we conclude, a) the asymmetric and symmetric frontal source coordinates are consistent with each other in the sense that the forced symmetry solution approximated the average of the asymmetric results, and b) that any asymmetry in the temporo-parietal lobe is likely to be trivial by comparison with the frontal lobe asymmetry. However, it remains to be shown whether the extension of source activity on the y axis could reflect an antero-posterior asymmetry of dipole location in the two hemispheres for which we were unable to find a stable solution.

As with the T1 solution, in the final T2 solution the right frontal lobe was activated first. This was followed by the other three sources in the left frontal and both temporal lobes, all about 20 ms later (fig. 3). The strength of the right temporal source was significantly smaller than any of the other 3 dipoles (t = -2.3 to −3.7, p = .04 − .003). Confirming the previously described increased Nd peak latency, dipole latencies tended to be later in T2 (especially the 2 sources in the left hemisphere, t = 2.1, p = .057). Sources tended to be non-significantly stronger in the T2 session vs. T1 (e.g. left frontal dipole, t = 2.05, p = .062), but were strikingly correlated (r = .66-.69, p =.009-.015), with the marked exception of the weaker right temporal lobe dipole (t = -2.8, p = .015).

### Summary

In the time dimension Nd onset varied by 56 ms (164 −220 ms), and peak latency by 40 ms (184-224 ms) between individuals. Between sessions the mean peak latency increased by only 14 ms (205-219 ms), while for the 4 dipole sources mean latencies were delayed by 4-16 ms in session 2. For the 3 spatial dimensions, we estimate that a volume of no more than 5 mm diameter within the mid-frontal gyrus on the right, and the superior frontal gyrus on the left represent the extent of tissue providing the active sources of the two frontal dipoles. This estimate also reflects the error of measurement and of the inverse solution calculation (see discussion below). In the temporal lobe there appears to be a more extensive plateau of activation of only 0.5 cm in depth, that extends up to 2 cm laterally, and 3 cm posteriorly. We suggest that the extent of the area of the auditory association cortex activated on the temporal- parietal-occipital borders may explain why the apparent dipole point strength was about half that recorded for the frontal sources.

### DISCUSSION

This is the first report of the putative localisation of the dipole sources of activity in the brain elicited by the event-related potential called the negative difference (Nd). This is an indicator of activity associated with controlled attention processes. The first source lies in a right frontal region (BA10) before activity spreads to BA 8 on the left and the temporo-parietal-occipital borders in both hemispheres.

Both frontal and temporo-parietal Nd sources are active *after* the detection of auditory deviance, marked by the MMN, and are located in different areas of the brain (Jemel et al. 2002). Not a single value of MMN ERP peak or dipole latency overlapped with the values for Nd. The strength of the findings reported here lies first in the specificity to process (Nd *vs*. MMN), second in the replication of the dipole solution after a month, and third with an investigation of the extent of the area delimiting the activity recorded (the physiological precision of the inverse solution).

### Methods

As Nd depends on the target-related associations of a stimulus, the process of controlled selective attention indexed by Nd

here should be pertinent to other discriminations at least within the auditory modality. Important perceptual features included the use of salient auditory stimuli to enhance signal-to-noise ratios, and a vigilance task to balance the baseline between conditions. All stimuli were binaurally presented. Clearly the use of unilateral presentations would lead to differences in processing measures, and possibly dipole localisation in the two hemispheres.

How specific is the Nd ERP to the proposed underlying process? First, the ERP and dipole latency differences between N1, MMN and Nd suggest a minimal direct contribution of the earlier events to Nd. Secondly, the computation of radial SCD maps facilitated interpretation of potentially overlapping sources (Alcaini et al. 1995; Pernier et al. 1988). Thirdly, studies of the frontal contributions to Nd depend on ERP measures: magnetoencephalographic methods are sensitive only to tangential currents in the sulci and not to the radial currents in the cortical gyri (Hamäläinen et al. 1993; Rinne et al. 2000). Lastly, the subtraction process used to derive the Nd controls for all the other stimulus-related effects apart from the direct association of the stimulus to its designation as a target.

What is the spatial accuracy of BESA ERP analysis? Studies on the accuracy of models of superficial and deep dipoles with 19-64 electrode arrays imply a localisation error of 3 (superficial sites) to 12 mm (deep sites) using 32 leads (Yvert et al. 1997). This may increase to 20 mm for deep sources and poor signal-to-noise ratios (Laarne et al. 2000). Our step-by-step analysis revealed a remarkable consistency of fit for 1 mm moves within source regions and a notable instability for 1 mm moves at their borders. This accuracy matches BESA values reported for processing negativity in the temporal and frontal lobes (2-4 mm, respectively, van der Stellt et al. 2001). Considering that Crottaz-Herbette and Ragot (2000) also reported a localisation error of ca.10 mm, we posit an error after our step-by-step analysis (taking in to account the number of electrodes, signal-to-noise ratio, and accuracy of the inverse solution) of the

order of 5-10 mm or less. (But this estimate does not include any error arising from use of the Montreal brain atlas on a particular individual.) This error is about twice that attributed to haemodynamic methods (Cabeza and Nyberg, 2000). As the equivalent current dipole approach of BESA assumes a small number of focal sources, it is more precise than the low resolution approach of LORETA (ca.15 mm: Gallinat et al. 2002) that inadequately accounts for inter-individual variability and suffers from a smoothness constraint rendering the distinction of activity in neighbouring areas difficult. While records from >64 sites can yield enormously better topographic resolution (Gevins et al. 1999) dipole models based on increases from 18-64 sites achieve much more modest improvements (Laarne et al. 2000). Thus, an enhanced resolution (and reliability) will depend more on the digital integration of electrode location with head landmarks for each individual, and localising these on their own MRI anatomical images and to a custom-fitted head model.

### The Nd ERP component: the psychological process

Näätänen (1990) encouraged the distinction between processing negativity based on the target/standard comparison and Nd based on ERPs from the _same_ stimulus in the target/non-target comparison. This paved the way for a precise attribution of function to the auditory and visual Nd, avoiding the effects of perceptual differences between stimuli. Eimer (1996) showed that an Nd component was enhanced more by selective than sustained attention. Alho et al. (1994) showed Nd to be more pronounced during effortful _within_ channel comparisons of stimuli than in inter-modal attention conditions. Thus, the functional emphasis was placed on the conscious effort of selection and focussing of information processing. As an illustration of this, while MMN and P3 components may decrease with age, the activation of controlled attention may maintain or actually increase the size of Nd in the elderly (Karayanidis et al. 1995). Later Nd components are associated with rehearsal and maintenance of the attentional trace necessary for maintaining a correct discrimination (Kasai et al. 2001).

Woods and Alain (2001) showed that the processing of features contributing to Nd began during the MMN latency window, but the conjunction of attended features elicited negativity later (in the latency window studied here). This is consistent with our data that we propose shows controlled attention taking over from automatic change detection. The right frontal MMN dipole occurred 25 ms after those in the temporal lobe and in the same range as the earliest Nd dipole, also in the right frontal cortex (143-188 ms *vs.* 186 –196 ms respectively). Thus suggests that there may be sequential activation for processing a deviant target stimulus in BA 10 between the right inferior frontal (MMN) and the medial frontal gyri (Nd). This could fit a sequence from registering 'changed stimulus' (MMN) to 'changed relevance' (Nd), prior to the necessary planning (left frontal locus) and trace comparator processes (temporo-parietal loci). We now consider Nd-source loci for evidence for this proposal.

### The Nd ERP: sources – review of Nd locus and regional function

Knight and colleagues (1981; Woods and Knight, 1986) showed that left and (more so) right frontal brain-damage impaired Nd and the ability to attend and suppress distraction (see also the review by Viggiano, 1997). Later topographic analyses showed that various processing negativities could be detected in the auditory cortex (Hari et al. 1989), anterior to N1 sources (Rif et al. 1991) as well as in frontal regions (Okita, 1989) and especially in the "amodal anterior medial" frontal cortex (Woods, 1990). More precise MEG studies then placed Nd *posterior* to that for the N1 in primary sensory areas: the anterior medial frontal cortex was also shown to contribute (Näätänen and Picton, 1986; Arthur et al. 1991). Recent source current density analyses from 128 sites reported temporal lobe sources in the latency range we studied (Kasai et al.1999). However, their later component (>300 ms) was attributed to the medial frontal gyrus – that we found to be active 100 ms earlier.

Indeed, 3 temporal components have been described by Giard et al. (2000). Our results agree that the Nd2 (110-275 ms) reflects sources that are spatially separate from excitatory components (e.g. N1: auditory cortex). But we differ on two counts. First, we found the right frontal lobe was activated before (not after) the auditory cortical Nd source. This is consistent with the re-activation from higher order centres of sensory areas reported for the visual system during focussed attention (Kastner and Ungerleider, 2000). Second while the Nd response can be stronger in the left hemisphere (e.g. session T2), as Giard et al maintain, this is not a reliable characteristic (session T1).

What parts of the frontal lobe showed Nd-related activity? Release (in T2) from the constraints and quasi-average solution of T1 revealed that the right hemisphere source was more antero-ventral (mid-frontal BA 10) than the left hemisphere source (superior frontal BA8). The former has been associated with the integration of figural information (Kounios et al. 2001) and in 6 neuroimaging studies with recognition, matching and working memory processes involved in problem-solving (e.g. card-sorting, Tower-of-London, Ravens-figures: review, Cabeza and Nyberg, 2000). In contrast, BA 8 on the left is activated during orienting, conceptual priming, encoding during distraction and dual task conditions, (6 reports in Cabeza and Nyberg 2000). All of these variables would necessarily be involved in the visuo-auditory presentation that we used. The one study that reported activation of both of these frontal regions, as well as temporo-parietal regions (including BA 39), was an investigation of sustained visual spatial attention and working memory (Coull et al. 1996: PET).

Studies of brain damage are also consistent with the present description of temporo-parietal Nd sources. Verleger et al. (1997) studied tone discrimination in 9 patients with right parietal lesions. In 6 of these damage encroached on the temporal lobe. Overall frontal and parietal records showed reduced Nd amplitude. Further, Woods et al. (1993) reported that temporo-parietal damage decreased Nd amplitude bilaterally, and specific damage in the inferior parietal region abolished the Nd ipsilaterally.

The posterior extension of "temporal lobe" sources to the parietal and occipital borders is *a priori* plausible as <u>conscious</u> attention-related processes are more likely to be more apparent in higher association areas than in primary sensory regions. This is supported by the reported *decrease* of primary auditory cortex activity associated with the process of training to make a difficult auditory tone discrimination (Jäncke et al. 2001: fMRI). It is also pertinent that both Gitelman et al. (1999) and Corbetta and Schulman (2003) defined a network of regions where activity related to controlled visual selective attention processes that border on the posterior area identified in this Nd study. These regions ranged from the intra-parietal sulcus and precuneus to posterior infero-temporal regions (BA 21, 37) and the superior temporal-parietal junction (BA 22, 40). Finally, the posterior extension described here for auditory data may parallel a ventral extension described for the visual modality. In that case, the progress from early Nd to later "selection negativity" during visual spatial frequency discrimination moved from dorsal extrastriate areas to ventral extrastriate fusiform cortex (Martinez et al. 2001).

### Neuroimaging after auditory stimulation

Neuroimaging reports are broadly consistent on the localisation of regions active in auditory discrimination. For example, tone discriminations elicit activity bilaterally in both prefrontal and mid-temporal regions (Zatorre et al. 1998, fMRI). A recent comparison of responses to novel and familiar tones reported activity in 2 temporo-parietal loci slightly lateral to the area reported here; the one just dorsal and the other just ventral (BA22, 37: Downar et al. 2002: fMRI). Lahti et al. (2001, PET) reported a right mid-frontal activation similar to our own on an effortful tone discrimination. Superior-medial frontal sources on the borders of BA8/9/10 were found in sustained attention tasks involving the counting of clicks. These were slightly medio-dorsal to the sources reported here on the right, but reminiscent of our quasi-average solution under symmetry constraints (Ortuno et al. 2002; Ojeda et al. 2002, PET studies).

Nonetheless several imaging studies report sources of auditory activity in other regions.

The reason is often that these studies do not have the time resolution to distinguish events that parallel the stages of processing reflected by ERP components. For example, one might have expected studies of auditory working memory and match to sample tasks (Alain et al. 2001, fMRI and ERP; Menon et al. 2001, fMRI) to report active loci similar to those that we found. Instead, the coordinates suggest a similarity to those described for MMN (Jemel et al. 2002). Similar results were found from an oddball presentation with no task component (Dittmann-Balcar et al. 2002, PET). Activity was reported in the superior temporal gyrus (where N1 dipoles are known), the inferior frontal gyrus (where MMN dipoles are known) and in the mid- and superior frontal gyri (where we report Nd dipoles). But if a discrimination is required, active regions also involve mid- and superior frontal gyri (as with the Nd here), and the anterior cingulate and inferior frontal regions (reported for MMN) among other clusters of activity (e.g., Kiehl et al. 2001; Müller et al. 2001: fMRI)

### Auditory processing: the temporal sequence of activation

Sources for the excitation of primary auditory cortex by salient tones (N1, at c. 100-110 ms) occur 1-2 cm anterior to the Nd activity described here: but, the x and z coordinates are similar. ERP dipoles reflecting change-detection (MMN) occur in between N1 and Nd loci, some 20-40 ms after the N1 sources. Temporo-parietal sources for Nd are active a further 1 cm more caudally, and are active after the frontal sources for MMN and Nd (frontal maxima 180-190 ms, temporo-parietal 200-220 ms): i.e. frontal change-detection precedes Nd-related attentive processes. The right inferior-frontal and left anterior cingulate MMN generators are active a bit earlier than the mid-frontal Nd source on the right. (Precise latencies for maximum dipole activity depend on the nature of the deviant stimulus [c. 120-200 ms]). Thereafter stimulus-related information is distributed with a similar delay (20-30 ms) to left superior frontal and temporo-parietal loci.

The "selective" functions represented in this circuit probably start with the detection of transient changes in the physical properties of

sounds (increased N1 amplitude, Opitz et al. 2002). In an ERP and fMRI study these authors reported loci within 10 mm of our data (Jemel et al. 2002), posterior to the N1. They interpret this as reflecting an MMN-related comparison of deviant mismatch with a working memory trace of the standard. They also reported right inferior frontal MMN activity, similar to Jemel et al. (2002). Based on the changes of response latency to stimuli following a deviant, the function of this frontal activity has been interpreted as an involuntary switch in the ongoing processing of information. This switch is regarded as an adaptive response to the mismatch registered in the temporal lobe. The potential function of the left cingulate dipole is suggested by results from an fMRI study of the role of cues that did/did not provide information on the need for a switch of target selection (Luks et al. 2002). The anterior cingulate, rather than the dorsolateral prefrontal region was uniquely involved in the cue effects. The authors proposed a role for the cingulate locus in monitoring the preparatory allocation of attention. It would seem plausible for target discrimination (relevance detection), that right mid-frontal regions then be brought in to play (initial Nd activation) to direct integration and recognition. To facilitate continued appropriate orientation and processing during distraction, the left superior frontal (Nd-active) region becomes active at the same time as the matching-with-'target-ness', working-memory templates in (Nd-active) parieto-temporal regions.

This interpretation is based on the attributions considered necessary for performing the current auditory discrimination, and those used in neuroimaging studies of tasks with similar attentional requirements. Prominent examples are the frontal and temporo-parietal sources described in the imaging study of sustained attention (Coull et al.1996). But it should be noted that the necessary reciprocal fronto-temporal anatomical connections have been reported in Rhesus monkey and found to be active during focussed attention (Rempel-Clower and Barbas, 2000). Further, neurophysiological study has demonstrated the necessary involvement of both hemispheres in discrimination under executive control (e.g. the cue-prompted retrieval of *correct* stimuli from contralateral temporal lobe stores, Hasegawa et al. 1998).

***Conclusions***

This article reports on right mid-frontal and left superior frontal loci as well as temporo-parietal Nd sources involved in target selection in an auditory sustained attention task. These conscious controlled selective processes have been placed in the temporal context of the automatic detection and processing of stimulus change. While the present ERP study has produced results consistent with some emerging from haemodynamic imaging studies, the interpretations are based on the distinction of components only separable with ERP recording. It is therefore essential that they should be replicated with other source analyses.

**REFERENCES**

Alain, C., Arnott, S. R., Hevenor, S., Graham, S. and Grady, C. L. "What" and "Where" in the human auditory system. Proc. Natl. Acad. Sci. (USA), 2001, 98: 12301-12306.

Alcaini, M., Giard, M-H., Echallier, J-F. and Pernier, J.F. Selective auditory attention effects in tonotopically organized cortical areas: a topographic ERP study. Hum. Brain Mapp., 1995, 2: 159-169.

Alho, K., Woods, D. L. and Algazi, A. Processing of auditory stimuli during auditory and visual attention as revealed by event-related potentials. Psychophysiology, 1994, 31: 469-479.

Arthur, D. L., Lewis, P. S., Medvick, P. A. and Flynn, E. R. A neuromagnetic study of selective auditory attention. Electroencephalogr. Clin. Neurophysiol., 1991, 78: 348-360.

Cabeza, R. and Nyberg, L. Imaging cognition II: an empirical review of 275 PET and fMRI studies. J. Cogn. Neurosci., 2000, 12: 1-47.

Corbetta, M. and Shulman, G. L. Control of goal-directed and stimulus-driven attention in the brain. Nature Rev. Neurosci. 2003, 3: 201-215

Coull, J. T., Frith, C. D., Frackowiak, R. S. J. and Grasby, P. M. A fronto-parietal network for rapid visual information processing. A PET study of sustained attention and working

memory. Neuropsychologia, 1996, 34: 1085-1095.

Cowan, N., Winkler, I., Teder, W. and Näätänen, R. Memory prerequisites of mismatch negativity in the auditory event-related potential (ERP). J. Exp. Psychol. Learn. Mem. Cog. 1993, 19: 909-921.

Crottaz-Herbette, S. and Ragot, R. Perception of complex sounds: N1 latency codes pitch and topography codes spectra. Electroencephalogr. Clin. Neurophysiol., 2000, 111: 1759-1766.

Deouell, L.Y., Bentin, S. and Giard, M-H. Mismatch negativity in dichotic listening: evidence for inter-hemispheric differences and multiple generators, Psychophysiology, 1998, 35: 355-365.

Dien, J., Tucker, D.M., Potts, G. and Hartry-Speiser, A. Localization of auditory evoked potentials related to selective attention, J. Cogn. Neurosci., 1997, 9: 799-823.

Dittmann-Balcar, A., Jüptner, M., Jentzen, W. and Schall, U. Dorsolateral prefrontal cortex activation during automatic auditory-duration mismatch processing in humans: a positron emission tomography study. Neurosci. Lett., 2001, 308**:** 119-122.

Downar, J., Crawley, A. P., Mikulis, D. J. and Davis, K. D. A cortical network sensitive to stimulus salience in a neutral behavioral context across multiple sensory modalities. J. Neurophysiol., 2002, 87: 615-620.

Eimer, M. ERP modulations indicate the selective processing of visual stimuli as a result of transient and sustained spatial attention. Psychophysiology, 1996, 33: 13-21.

Escera, C., Alho, K., and Schröger, E. and Winkler, L. Involuntary attention and distractibility as evaluated with event related potentials. Audiol. Neurootol., 2000a, 5: 151-166.

Escera, C., Yago, E., Polo, M.D. and Grau, C. The individual replicability of mismatch negativity at short and long inter-stimulus intervals. Clin. Neurophysiol., 2000b, 111: 546-551.

Gallinat, J., Mulert, C., Bajbouj, M., Herrmann, W. M., Schunter, J., Senkowski, D., Moukhtieva, R., Kronfeldt, D. and Winterer, G. Frontal and temporal dysfunction of auditory stimulus processing in schizophrenia. Neuroimage, 2002, 17: 110-127.

Gevins, A., Smith, M. E., McEvoy, L. K., Leong, H. and Le J. Electroencephalographic imaging of higher brain function. Phil. Trans. R. Soc. Lond. B, 1999, 354: 1125-1134.

Giard, M-H., Fort, A., Mouchetant-Rostaing, Y. and Pernier, J. Neuro-physiological mechanisms of auditory selective attention in humans. Front. Biosci. 2000, 5: 84-94.

Gittelman, D. R., Nobre, A. C., Parrish, T. B., LaBar, K. S., Kim, Y-H., Meyer, J. R. and Mesulam, M-M. A large scale distributed network for covert spatial attention: Further anatomical delineation based on stringent behavioural and cognitive controls. Brain, 1999, 122: 1093-1106.

Hamäläinen, M., Hari, R., Ilmoniemi, R. J., Knuutila, J. and Lounasmaa, O. V. Magnetoencephalography – theory, instrumentation, and application to non-invasive studies of the working human brain. Rev. Mod. Phys., 1993, 65: 413-498.

Hansen, J. C., and Hillyard, S. A. Endogenous brain potentials associated with selective auditory attention. Electroencephalogr. Clin. Neurophysiol., 1980, 49: 277-290.

Hansen, J. C., and Hillyard, S. A. Attention to multidimensional auditory stimuli. J. Exp. Psychol. Hum. Percept. Perform., 1983, 9: 1-19

Hari, R., Hamäläinen, M., Kaukoranta, E., Makela, J. P., Joutsiniemi, S-L. and Tiihonen, J. Selective listening modifies activity of the human auditory cortex. Exp. Brain Res., 1989, 74: 463-470.

Hasegawa, I., Fukushima, T., Ijhara, T. and Miyashita, Y. Callosal window between prefrontal cortices: cognitive interaction to retrieve long-term memory. Science, 1998, 281: 814-818.

Hillyard, S. A. and Picton, T. W. Electrophysiology of cognition. In, F. Plum and V.B. Mountcastle, (Eds.). Handbook of Physiology: The Nervous System. American Physiological Society, Bethesda, MD, 1988: 519-583.

Jäncke, L., Gaab, N., Wustenberg, T. Scheich, H. and Heinze, H. J. Short-term functional plasticity in the human auditory cortex: an fMRI study. Cog. Brain Res. 2001, 12: 479-485.

Jemel, B., Achenbach, C., Wiemer, P., Röpcke, B. and Oades, R. D. Auditory frequency- and duration-deviant detection elicits similar asymmetrical dipole sources localised in both the temporal lobe and in the frontal cortices. Neuroimage, 2001, 13: 323.

Jemel, B., Achenbach, C., Müller, B. W., Röpcke, B. and Oades, R. D. Mismatch negativity results from bilateral asymmetric dipole sources in the frontal and temporal lobes. Brain Topogr. 2002, 15: 13-27.

Kamijo, K-I., Yamazaki, T., Kiyuna, T., Takaki, Y. and Kuroiwa, Y. Visual event-related potentials during movement imagery and the dipole analysis. Brain Topogr. 2002, 14: 279-292.

Karayanidis, F., Andrews, S., Ward, P. B. and Michie, P. T. 1995. ERP indices of auditory selective attention in aging and Parkinson's disease. Psychophysiology, 1995, 32: 335-350.

Kasai, K., Nakagome, K., Itoh, K., Koshida, I., Fukuda, M., Watanabe, A., Kamio, S., Murakami, T., Hata, A., Iwanami, A., Hiramatsu, K-I. and Kato, N. Electro-physiological evidence for sequential activation of multiple brain regions during the auditory selective attention process in humans. NeuroReport, 1999, 10: 3837-3842.

Kasai, K., Nakagome, K., Iwanami, A. and Fukuda, M. Neuropsychiatry and the auditory selective attention process. Curr. Opin. Psychiatry, 2001, 14: 219-225.

Kastner, .S, and Ungerleider, L. G. Mechanisms of visual attention in the human cortex. Ann. Rev. Neurosci., 2000, 23: 315-341.

Kiehl, K.A., Laurens, K.R., Duty, T.L., Forster, B.B. and Liddle, P.F. Neural sources involved in auditory target detection and novelty processing: an event-related fMRI study. Psychophysiology, 2001, 38: 133-142.

Knight, R. T., Hillyard, S. A., Woods, D. L. and Neville, H. J. The effects of frontal cortex lesions on event-related potentials during auditory selective attention. Electroencephalogr. Clin. Neurophysiol., 1981, 52: 571-582.

Kounios, J., Smith, R.W., Yang, W., Bachman, P. and D'Esposito, M. Cognitive association formation in human memory revealed by spatiotemporal brain imaging. Neuron, 2001, 29: 297-306.

Laarne, P.H., Tenhunen-Eskelinen, M. L., Hyttinen, J. K. and Eskola, H. J. 2000. Effect of EEG electrode density on dipole localization accuracy using two realistically shaped skull resistivity models. Brain Topogr., 2000, 12: 249-254.

Lahti, A. C., Holcomb, H. H., Medoff, D. R., Weiler, M. A., Tamminga, C. A. and Carpenter, W. T. Abnormal patterns of regional cerebral blood flow in schizophrenia with primary negative symptoms during an effortful auditory recognition task. Am. J. Psychiatry., 2001, 158: 1797-1808.

Lehmann, D. and Skrandies, W. Spatial analysis of evoked potentials in man – a review. Prog. Neurobiol., 1984, 23:227-250.

Luks, T. L., Simpson, G. V., Feiwell, R. J. and Miller, W. L. Evidence for anterior cingulate cortex involvement in monitoring preparatory attentional set. Neuroimage, 2002, 17: 792-802.

Martinez, A., Di Russo, F., Anllo-Vento, L. and Hillyard, S. A. Electrophysiological analysis of cortical mechanisms of selective attention to high and low spatial frequencies. Clin. Neurophysiol., 2001, 112: 1980-1998.

Menon, V., Anagnoson, R. T., Mathalon, D. H., Glover, G. H. and Pfefferbaum, A. Functional neuroanatomy of auditory working memory in schizophrenia: relation to positive and negative symptoms. Neuroimage, 2001, 13: 433-446.

Müller, R-A., Kleinhans N. and Courchesne, E. Broca's area and the discrimination of frequency transitions: a functional MRI study. Brain Lang., 2001, 76: 70-76.

Näätänen, R. Implications of ERP data for psychological theories of attention. Biol. Psychol., 1988, 26: 117-163.

Näätänen, R. The role of attention in auditory information processing revealed by event-related potentials and other measures of cognitive function. Behav. Brain Sci, 1990, 13: 201-288.

Näätänen, R. and Picton, T. W. N2 and automatic versus controlled processes. Electroencephalogr. Clin. Neurophysiol., 1986, 38: (supplement) 169-186.

Nunez P. L. Electric fields of the brain. Oxford University Press, New York, 1981.

Nunez, P. L., Silberstein, R. B., Cadusch, P. J.,

Wijesinghe, R. S., Westdorp, A. F. and Srinivasan, R. A theoretical and experimental study of high resolution EEG based on surface Laplacian and cortical imaging, Electroencephalogr. Clin. Neurophysiol., 1994, 90: 40-57.

Oades, R. D., Dittmann-Balcar, A. and Zerbin, D. The topography of 4 subtraction ERP-waveforms derived from a 3-tone auditory oddball task in healthy young adults. Int. J. Neurosci., 1995, 81: 265-281.

Oades, R. D., Ditmann-Balcar, A., and Zerbin, D. Development and topography of auditory event-related potentials (ERPs): Mismatch and processing negativity in individuals 8-22 years of age. Psychophysiology, 1997, 34: 677-693.

Oades, R. D., Zerbin, D., Dittmann-Balcar, A. and Eggers, C. Auditory event-related potential (ERP) and difference wave topography in schizophrenic patients with/without active hallucinations and delusions: a comparison with young obsessive-compulsive disorder (OCD) and healthy subjects. Int. J. Psychophysiol. 1996, 22: 185-214.

Okita, T. Within channel selection and event-related potentials during auditory selective attention. Psycho-physiology, 1989, 26: 127-139.

Ojeda, N., Ortuno, F., Arbizu, J., Lopez, P., Marti-Clement, J. M., Penuelas, I., and Cervera-Enguix, S. Functional anatomy of sustained attention in schizophrenia: contribution of parietal cortices. Hum. Brain Mapp., 2002, 17: 116-130.

Opitz, B., Rinne, T., Mecklinger, A., von Cramon, D. Y. and Schröger, E. Differential contribution of frontal and temporal cortices to auditory change detection: fMRI and ERP results. Neuroimage, 2002, 15: 167-174.

Ortuno, F., Ojeda, N., Arbizu, J., Lopez, P., Marti-Climent, J. M., Penuelas, I. and Cervera, S. Sustained attention in a counting task: normal performance and functional neuroanatomy. Neuroimage, 2002, 17: 411-420.

Pasqual-Marqui, R. D. and Lehmann, D. Topographic maps, source localization, and the reference electrode: comments on a paper by Desmedt et al. Electroencephalogr. Clin. Neurophysiol.,

1993, 88: 530-533.

Pernier, J., Perrin, F., and Bertrand, O. Scalp current density fields: concept and properties. Electroencephalogr. Clin. Neurophysiol., 1988, 69: 385-389.

Picton, T. W., Lins, O. G. and Scherg, M. The recording and analysis of event-related potentials. In F. Boller and J. Grafman (Eds), Handbook of Neuropsychology, Elsevier, Amsterdam, 1995: 3-73.

Rempel-Clower, N.L. and Barbas, H. 2000. The laminar pattern of connections between prefrontal and anterior temporal cortices in the Rhesus monkey is related to cortical structure and function. Cereb. Cortex, 2000, 10: 851-865.

Rif, J., Hari, R., Hamäläinen, M. S. and Sams, M. Auditory attention affects two different areas in the human supratemporal cortex. Electroencephalogr. Clin. Neurophysiol. 1991, 79: 464-472.

Rinne, T., Alho, K., Ilmoniemi, R.J., Virtanen, J. and Näätänen, R. Separate time behaviors of the temporal and frontal mismatch negativity sources. Neuroimage, 2000, 12: 14-19.

Scherg, M. and Berg, P. Use of a priori knowledge in brain electromagnetic brain activity. Brain Topogr., 1991, 4: 143-150.

Scherg, M. and Picton, T. W. Separation and identification of event-related brain potential components by brain electric source analysis. Electroencephalogr. Clin. Neurophysiol., 1991, Suppl. 42: 24-37.

Sussman, E., Winkler, I., Kreuzer, J., Saher, M., Näätänen, R. and Ritter, W. Temporal integration: intentional sound discrimination does not modulate stimulus-driven processes in auditory event synthesis. Clin. Neurophysiol., 2002, 113: 1909-1920.

Treisman, A. M. Strategies and models of selective attention. Psychol. Rev., 1969, 76: 282-299.

Van der Stellt, O., van der Molen, M., Gunning, W. B. and Kok, A. Neuroelectric signs of selective attention to color in boys with attention-deficit hyperactivity disorder. Cog. Brain Res., 2001, 12: 245-264.

Verleger, R., Heide,W., Butt, C., Wascher, E. and Kömpf, D. On-line brain potential correlates of right parietal patients' attentional deficit. Electroencephalogr. Clin

Neurophysiol., 1997, 99: 444-457.

Viggiano, M. P. Event-related potentials in brain-injured patients with neuro-psychological disorders: a review. J. Clin. Exp. Neuropsychol., 1997, 18: 631-647.

Waberski, T. D., Kreitschmann-Andermahr, I., Kawohl, W., Farvas, F., Ryang, Y., Gobbele, R. and Buchner, H. Spatio-temporal source imaging reveals subcomponents of the human auditory mismatch negativity in the cingulum and right inferior temporal gyrus. Neurosci. Lett., 2001, 308: 107-110.

Woods, D. L. 1990. The physiologic basis of selective attention: implications of event-related potential studies. In: R. Pasuraman, and R. Johnson (Eds), Event-related brain potentials: basic issues and applications, Oxford University Press, N.Y, New York, 1990: 178-209

Woods, D.L. and Alain, C. Conjoining three auditory features: an event-related brain potential study. J. Cogn. Neurosci., 2001, 13: 492-509.

Woods D. L. and Knight, R. T. Electro-physiologic evidence of increased distractibility after dorsolateral prefrontal lesions. Neurol., 1986, 36: 212-216.

Woods, D.L., Knight, R.T. and Scabini, D. Anatomical substrates of auditory selective attention: behavioral and electrophysiological effects of posterior association cortex lesions. Cogn. Brain Res., 1993, 1: 227-240.

Yvert, B., Bertrand, O., Thevenet, M., Echallier, J.F. and Pernier, J. A systematic evaluation of the spherical model accuracy in EEG dipole localization. Electroencephalogr. Clin. Neurophysiol., 1997, 102: 452-459.

Zatorre, R. J., Perry, D. W., Beckett, C. A., Westbury, C. F. and Evans, A. C. Functional anatomy of musical pro-cessing in listeners with absolute pitch and relative pitch. Proc. Natl. Acad. Sci (USA), 1998, 95: 3172-3177.